Pakistan Journal of Engineering and Technology, Pak JET
Multidisciplinary & Peer Reviewed
Volume: 4, Number: 2, Pages: 13- 20, Year: 2021

Experimental Investigation of Wing Accuracy Quantification using Point Cloud and Surface Deviation

Mehmood Ahmad[1], Sheharyar Nasir[1], Zia-ur Rahman[2], Shuaib Salamat[1], Umar Sajjad[3], Asad Raza[1]
1Air University, Aerospace and Aviation Campus, Islamabad
2National University of Science and Technology, Islamabad
3Illinois Institute of Technology, USA

Corresponding author: Mehmood Ahmad (e-mail: mehmood@aerospace.pk)

***Abstract*-A rapidly advancing lean production industry demands quick manufacturing solutions with greater precision and accuracy. This paper proposes a framework for the accurate quantification of a die-casted wing using laser scanning and reverse engineering technique. In this technique, the wing upper and lower surfaces are scanned using a Coordinate Measuring Machine (CMM). This scanned data is then imported into CAD software to generate the surface using Free Form Reverse Engineering (FFRE). The model fitness test patronizes the curve fitting used for the surface generation. The generated surface and the original 3D CAD model are investigated using deviation analysis for inaccuracies originating due to manufacturing and data acquisition. The wing is further analyzed by the point data to 3D CAD model deviation analysis. The methodology adopted significantly minimizes the data acquisition and data processing error allowing deviation to be solely traced back to the manufacturing technique.**

***Index Terms*: Accuracy quantification; Curve fitting, Deviation analysis; Free Form Reverse Engineering (FFRE); Model fitness test; Point cloud;**

I. INTRODUCTION

Today's Cutting-edge needs have considerably improved the outdated product developing techniques in modern manufacturing processes. In the last few decades, reverse engineering has emerged as a technically proven method for manufacturing; especially in the tool, die and mould making industries. Reverse engineering has also facilitated the manufacturing of automotive and aircraft components. The reverse engineering process comprises of data digitization of existing parts with digital systems and computer software for visualization, then converting digitized data into CNC readable format for manufacturing of duplicate parts [1, 2]. Swiftly growing markets require short development times for intricate and novel engineering parts to have an edge over the competitors. Reverse engineering in the current scenario plays a key role in the quick re-design of products with ergonomic features. Moreover reverse engineering is also employed to improve the existing design problems[3]. **Error! Reference source not found.** shows the key steps involved in reverse engineering [4].

Freeform reverse engineering is one type of reverse engineering process that deals with the creation of identical surface. Different stages involved in the free-form reverse engineering process are as follow:

a) Scanning object **b)** Data Cleaning **c)** Extracting contours, patches and grids **d)** Creating surfaces **e)** Verifying the surfaces **f)** Analyzing the accuracy of the surfaces **g)** Exporting final CAD model [5].

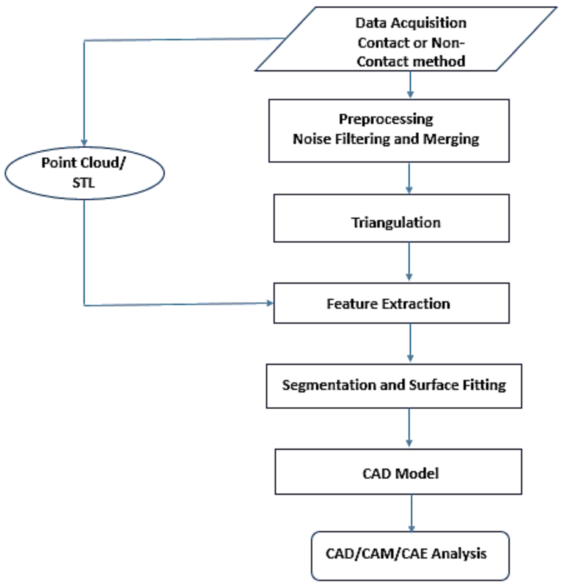

Figure 1 Reverse Engineering Flow Chart

Evaluation of geometric features using automatic measurement devices is increasingly being used in mass production [6]. Geometric features of any intricate physical model can be acquired by 3D scanning. The 3D scanned data represents a set of data points in the three-dimensional coordinate system. The scanned data produces an accurate representation of 3D objects [7]. 3D scanning is mainly characterized as a contact and non-contact procedure. The contact method as the name suggests is a method in which the measuring probe is in physical contact with the surface while scanning[5]. Point coordinates of the object are read using a contact probe. Non-contact scanning, such as a laser probe, involves no physical contact with the object being scanned. Laser probes produce an accurate and dense 3D point cloud in which in-depth detail of each surface feature is captured [8, 9]. Laser scanning technique is comparatively quick method to capture the surface[10]. The quality of scanned data points is highly dependent on the orthogonal positioning of the camera but independent of the distance between the object and the camera [11].

Curves and surfaces are extracted from the 3D scanned data of an object, then converted to a 3D CAD model for quality inspections and feature visualization. 3D scanned data is normally prone to machines errors and human errors. One such error, Noise, is a type of machine error that is induced due to the presence of gaps and bumpy surfaces introduced in a multitude of ways i.e. from extraneous vibrations, specular reflections, etc. Elimination of the noise in data samples is a particularly difficult task [12]. There are many different filtering approaches and tools that can be used to eliminate the scanned noise. A common technique is mesh gaps filling and smoothening.

The 3D scanned data can be obtained initially in the form of a point cloud or mesh file, but this point cloud data does not give a good insight of the errors and physical model, thus the 3D scan data is usually converted to mesh file (STL file) or NURBS surface for better visualization of features and errors [4, 13].

Different techniques are used to create a surface from scanned data. Peng and Loftus [1] used the shaded image from a digital camera for surface generation. Shaded Images were processed into CAD software readable format and were then exported to a CNC machine for new model generation. Tai and Huang [14] used the iterative method to generate 4^{th} order polynomial equation and removed noise points out of the range of regression equation within a predefined tolerance. Menq and Chen [15] used the iterative measurement algorithm to generate the refined surface from a 5^{th} order polynomial. Surfaces generated by any of the above-mentioned methods can be imported to CAD software for further analysis.

Deviation can be calculated by the Euclidian distance method, normal distance method or angle tolerance methods. Anil et al.[16] used the Euclidian distance and normal distance method to calculate the deviation of building structure. Due to its commonality, we incorporated the normal distance method in our study.

II. METHODOLOGY

Wing surfaces were generated using FFRE, to investigate, its upper and lower surface profiles. The steps were as follows:

A. Wing Scanning

The 3D coordinates were obtained from the physical model of the wing using a “CENTURY” coordinate measuring machine equipped with a “Renishaw PH10T” touch-trigger probe. Figure 2 represents the CMM machine along with the generated 3D scan data of the wing.

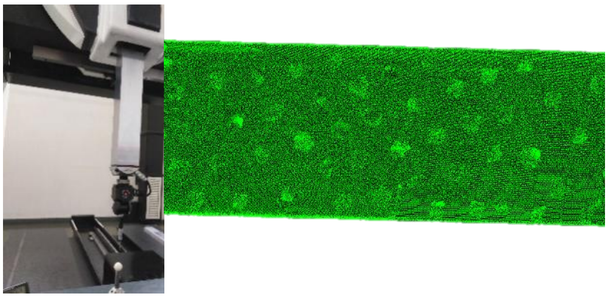

Figure 2 CMM with Scanned Wing Data

As seen in Figure 2, the 3D scan data contains inherent noise and gaps. This 3D scan data was then converted to a mesh file, for better visualization and removal of imperfections.

B. Mesh Refinement

After the mesh generation, imperfections such as gaps became obvious as seen in Figure 3.

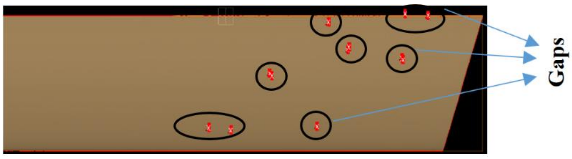

Figure 3 Gaps in Mesh Surface

These gaps were filled by creating triangular meshes which involves joining any three consecutive nodes in the vicinity of the gaps. This process resulted in the unevenness of the surface as seen in Figure 4.

Figure 4 Unevenness in Surface

In the refinement process, each triangular mesh was split down into sub meshes and optimized, resulting in mesh smoothness. The refined mesh is shown in **Error! Reference source not found.**.

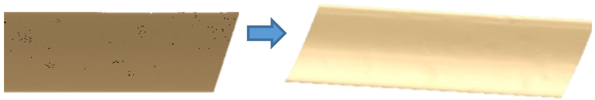

Before Refinement After Refinement

Figure 5 Refinement

C. Surface Generation

Span-wise planar sections were inserted on the refined mesh with a gap of 6mm to extract the curves. The extracted curves can be seen in Figure 6.

Figure 6 Curve Extraction

To accurately fit these curves requisite degree polynomial must be used depending on point distribution. The order of polynomial was determined by the model fitness test.

D. Model Fitness Test

A systematic methodology was adopted for the selection and validation of polynomial for the CAD generation process depending on the complexity of geometry. This methodology helps to minimize the error propagation, thus increasing the quality of the CAD model. Starting with a 2^{nd}-degree polynomial, three separate tests were conducted for each polynomial till the 8^{th} order. These tests were:

i. Actual by Predicted Value Test: To pass this test, predicted values must lie within the 95% confidence range of actual values. The plots for 2-8-degree polynomials are shown in Figure 8.

ii. Residual Plot Test: This test calculates the residual value and draws a plot between predicted and residual values.

$$Residual = Actual\ Value - Prdicted\ Value$$

To pass the test, the plot must be a gunshot and equally distributed about zero. The plots for 2-8-degree polynomials are shown in Figure 7. The coefficient of multiple determination (R^2) for each polynomial is also indicated in the residual plots.

iii. Error distribution Test: This test calculates the mean error and standard deviation of percentage error. To pass this test, the mean error must be close to zero and the standard deviation must be less than or equal to one. The mean error and standard deviation (SD) for each polynomial are shown in Table 1.

Table 1 Error Summary

	2^{nd} Degree	4^{th} Degree	6^{th} Degree	8^{th} Degree
Mean	9.39	0.78	0.13	0.07
SD	40.62	12.46	1.75	0.76

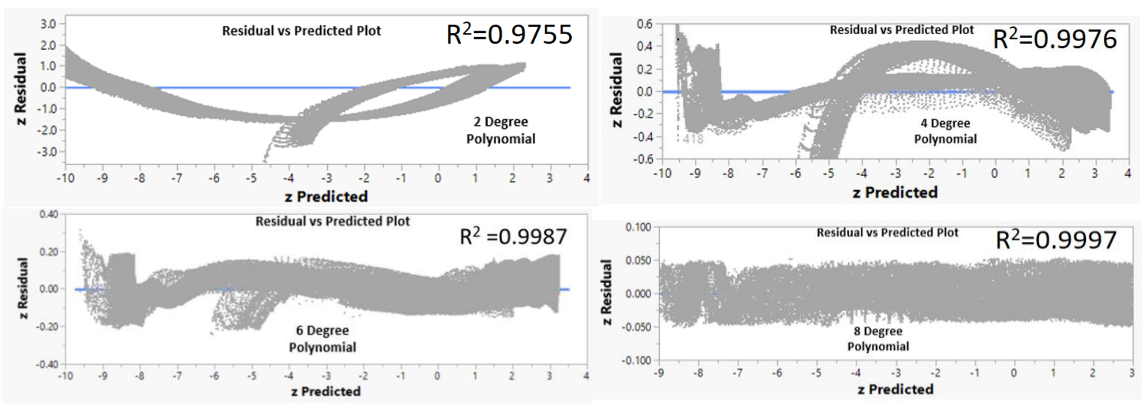

Figure 7 Residual vs Predicted Plot

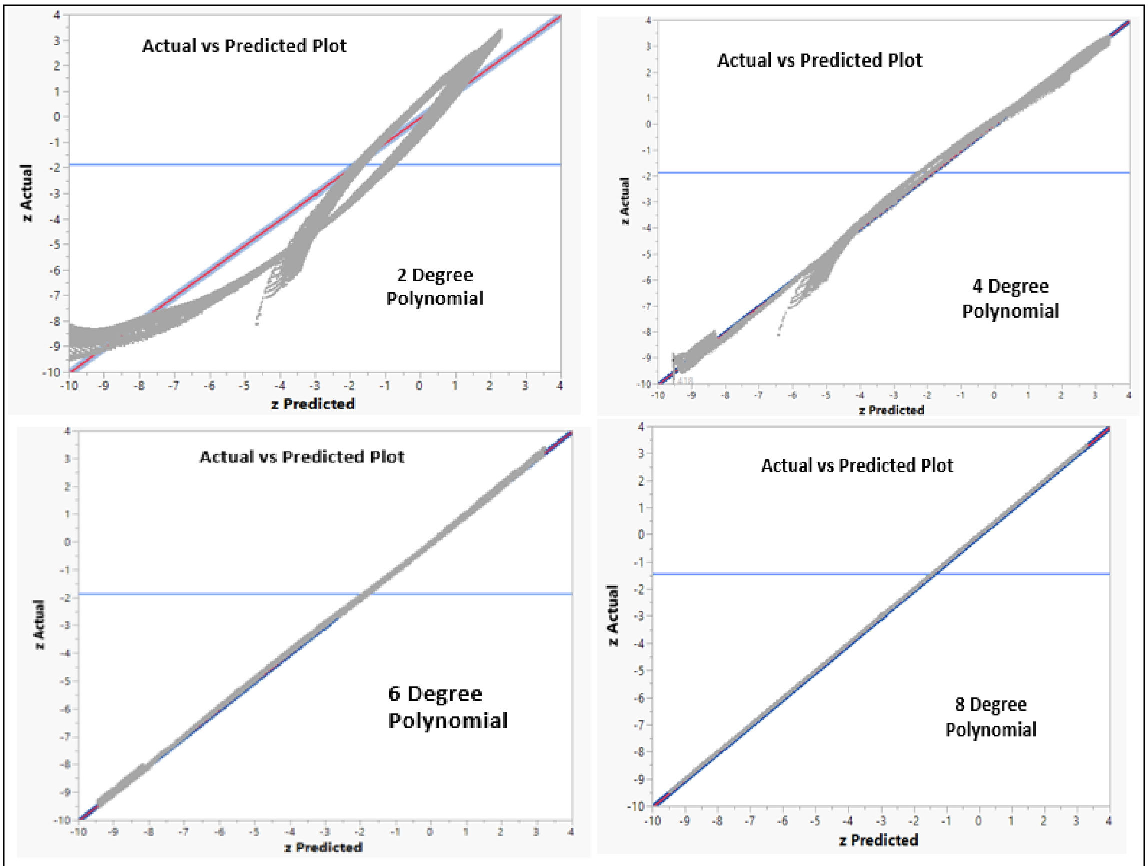

Figure 8 Actual vs Predicted Plot

E. Test Summary

Results of the three tests for each polynomial are tabulated in Table 2. It may be noted that the 8th-degree polynomial passes all the tests.

Table 2 Test Summary

	2nd Degree	4th Degree	6th Degree	8th Degree
Actual by Predicted Value Test	X	x	✓	✓
Residual Plot Test	X	x	x	✓
Error Distribution Test	x	x	x	✓

Therefore curve fitting was carried out using 8th order polynomial equation with 0.01mm tolerance and 0.025mm sag value. The Wing surface was generated using the curve fitting process which is shown in Figure 9.

Figure 9 Surface Generation

F. Surface Deviation

The deviation of generated wing surfaces was carried out with a 3D CAD model. The deviation analysis was performed in CAD software. The 3D CAD model and generated wing surface were ideally overlapped through several rotations and translations to ensure negligible miss placement error. The orthogonal distance from 3D CAD to generated wing surface was then calculated. Figure 10 shows the flow chart for deviation analysis.

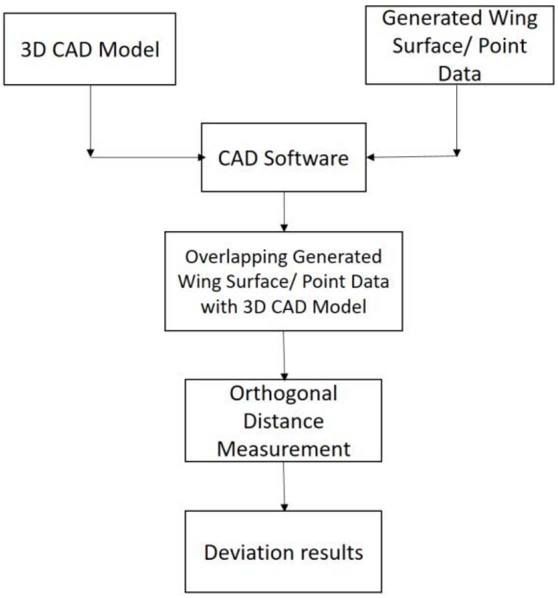

Figure 10 Deviation Analysis Flow Chart

The results for surface deviation analysis are summarized in Table 3 and also shown in Figure 11 and Figure 12.

III. POINT DATA DEVIATION

Wing upper and lower surfaces were further analyzed using point cloud data. The following methodology was adopted for point cloud data to CAD model deviation analysis.

A. Wing Division

For point data deviation analysis, the wing was divided into three regions along the chord on the upper and lower surface i.e. leading-edge, middle region and trailing edge. These regions were further divided into five segments of width 80mm spaced 150mm apart along the span. Names of the regions and their positions on the wing are mentioned in Table 4. Sample division is shown in Figure 13.

Table 3 Deviation Range using Surface to CAD Model

	Upper Surface	**Lower Surface**
Positive maximum deviation	0.096mm	0.359mm
Negative maximum deviation	-0.089mm	-0.168mm
Positive mean deviation	0.037mm	0.177mm
Negative mean deviation	-0.034mm	-0.116mm

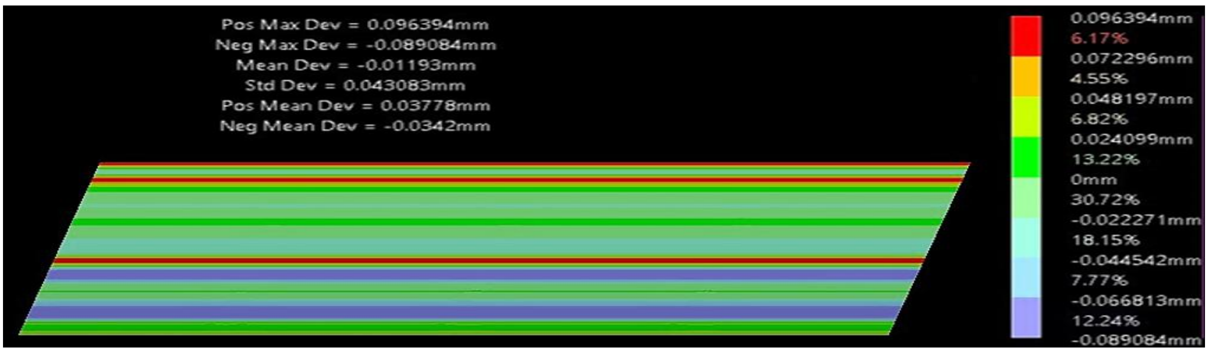

Figure 11 Wing Upper Surface to CAD Upper Surface Deviation

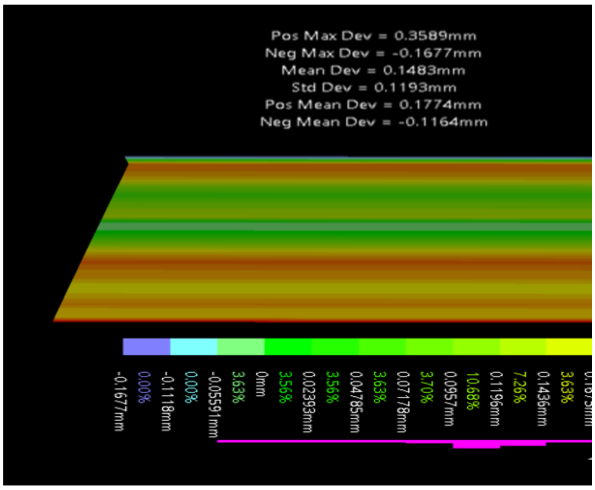

Figure 12 Wing Lower Surface to CAD Lower Surface Deviation

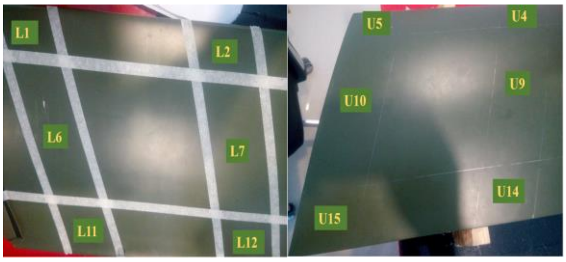

Figure 13 Upper and Lower Surface Region Marking

To get the point data of these regions, CMM was used. Point cloud data was acquired along the span and the chord in a regular pattern in these regions.

Table 4 Regions and their Position

No	Region	Position
1	U1,U2,U3,U4,U5	The Leading-edge portion of the upper surface
2	U6, U7, U8, U9, U10	The middle portion of the upper surface
3	U11,U12,U13,U14,U15	The trailing edge portion of the upper surface
4	L1, L2, L3, L4, L5	The leading-edge portion of the lower surface
5	L6,L7,L8,L9,L10	The Middle portion of the lower surface
6	L11,L12,L13,L14,L15	The trailing edge portion of the lower surface

B. Point Deviation Analysis

Point data obtained from CMM was compared with the respective regions of the 3D CAD model. For every region, the number of data points taken and deviation range is tabulated in Table 5 and also shown in Figure 14 and Figure 15.

Table 5 Deviation Range using Point Cloud to CAD Model

No	Region	Points Taken	Positive Max Deviation (mm)	Negative Max Deviation (mm)
1.	U1,U2,U3,U4,U5	≥120	0.192	-0.3
2.	U6,U7,U8,U9,U10	≥1200	0.319	-0.3
3.	U11,U12,U13,U14,U15	≥110	0.12	-0.32
4	L1,L2,L3,L4, L5	≥110	0.335	-0.17
5	L6,L7,L8,L9, L10	≥1100	0.335	-0.056
6	L11,L12,L13,L14,L15	≥110	0.335	Nil

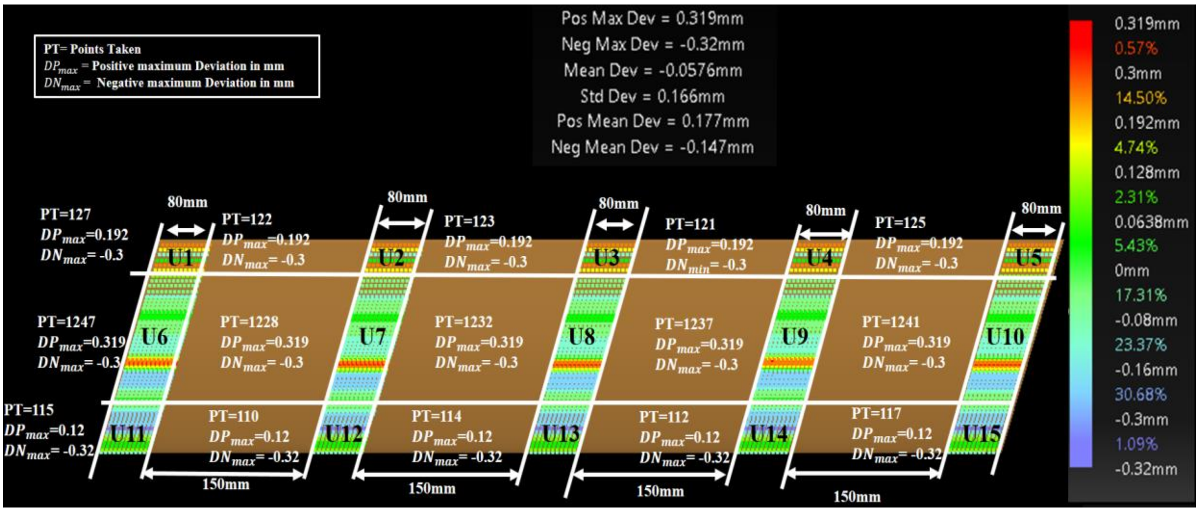

Figure 14 Wing Upper Surface Point Cloud Deviation Analysis

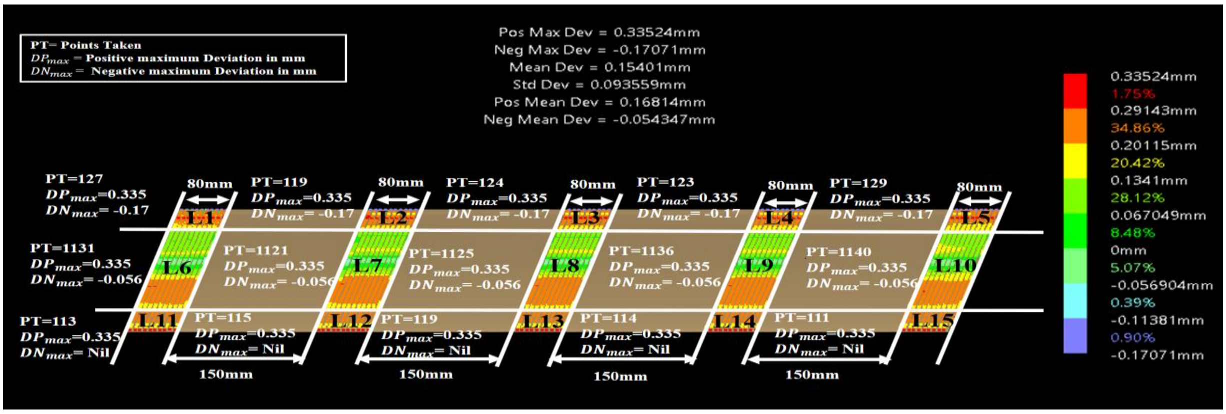

Figure 15 Lower Wing Surface Point Cloud Deviation Analysis

IV. CONCLUSION

The 3D point cloud data was obtained using CMM. After refinement, this data was used for the surface generation using the 8th-degree polynomial. Analysis shows that deviation of the upper surface using surface to CAD model had a range of +0.096mm to -0.089mm and point cloud to CAD model had a range of +0.319mm to -0.32mm. Similarly, the deviation of the lower surface using surface to CAD was in the range of +0.359mm to -0.168mm and point cloud to CAD was in the range of +0.335mm to -0.17mm. The results also validate the free form reverse engineering technique for a surface generation used in the study. The Surface generated after conducting the model fitness test was more accurate for deviation analysis, thus, confirming the robustness of the method.

REFERENCES

1. Peng, Q. and M.R. Loftus. *A new approach to reverse engineering based on vision information*. 1998.
2. Wang, J., et al., *A framework for 3D model reconstruction in reverse engineering.* 2012. **63**: p. 1189-1200.
3. Haleem, A., et al., *Redesign of Car Body by Reverse Engineering Technique using Steinbichler 3D Scanner and Projet 3D Printer.* Journal of Industrial Integration and Management, 2020: p. 2050007.
4. Kumar, A., P.K. Jain, and P.M. Pathak. *Industrial Application of Point Cloud / STL Data for Reverse Engineering*. 2012.
5. *Reverse engineering of physical objects – teaching manual*. 2004.
6. Kubátová, D., M. Melichar, and J. Kutlwašer, *Evaluation of Repeatability and reproducibility of CMM equipment.* Procedia Manufacturing, 2017. **13**: p. 558-564.
7. Moghaddame-Jafari, B., *Deflection Measurement through 3D Point Cloud Analysis*. 2017.
8. Pingbo Tang, B.A., Daniel Huber, *Characterization of Three Algorithms for Detecting Surface Flatness Defects from Dense Point Clouds.*
9. Gordon, S., et al., *Modelling point clouds for precise structural deformation measurement.* 2004. **35**: p. B5.
10. Bastas, A., *Comparing the probing systems of coordinate measurement machine: Scanning probe versus touch-trigger probe.* Measurement, 2020. **156**: p. 107604.
11. An, Z., *Accuracy Assessment of 3D Point Clouds Generated by Photogrammetry From Different Distances.* 2017.

12. Bogdan Rusu, Z.C.M., Nico Blodow, Mihai Dolha, Michael Beetz, *Towards 3D Point cloud based object maps for household environments.* Robotics and Autonomous Systems, 2008.

12. Khan, Muhammad Nasir, Hasnain Kashif, and Abdul Rafay. "Performance and optimization of hybrid FSO/RF communication system in varying weather." Photonic Network Communications vol. 41, no. 1, pp. 47- 56, 2021.

13. Jamil, Mohsin, Muhammad Nasir Khan, Saqib Jamshed Rind, Qasim Awais, and Muhammad Uzair. "Neural network predictive control of vibrations in tall structure: An experimental controlled vision." Computers & Electrical Engineering, vol. 89, pp. 106940, 2021.

14. Khan, Muhammad Nasir, Mohsin Jamil, Syed Omer Gilani, Ishtiaq Ahmad, Muhammad Uzair, and H. Omer. "Photo detector-based indoor positioning systems variants: A new look." Computers & Electrical Engineering, vol. 83, pp. 106607, 2020.

15. Kashif, Hasnain, Muhammad Nasir Khan, and Ali Altalbe. "Hybrid optical-radio transmission system link quality: link budget analysis." IEEE Access, vol. 8, pp. 65983-65992, 2020.

16. Khan, Muhammad Nasir, and Fawad Naseer. "IoT based university garbage monitoring system for healthy environment for students." In 2020 IEEE 14th International Conference on Semantic Computing (ICSC), pp. 354-358. IEEE, 2020.

17. Uzair, Muhammad, R. O. B. E. R. T. D DONY, Mohsin Jamil, KHAWAJA BILAL AHMAD MAHMOOD, and Muhammad Nasir Khan. "A no-reference framework for evaluating video quality streamed through wireless network." Turkish Journal of Electrical Engineering & Computer Sciences, vol. 27, no. 5, pp. 3383-3399, 2019.

18. Khan, Muhammad Nasir, Syed Omer Gilani, Mohsin Jamil, Abdul Rafay, Qasim Awais, Bilal A. Khawaja, Muhammad Uzair, and Abdul Waheed Malik. "Maximizing throughput of hybrid FSO-RF communication system: An algorithm." IEEE Access, vol. 6, pp. 30039-30048, 2018.

19. Khan, Muhammad Nasir, Syed K. Hasnain, and Mohsin Jamil. Digital Signal Processing: A Breadth-first Approach. Stylus Publishing, LLC, 2016.

20. Khan, Muhammad N. "Importance of noise models in FSO communications." EURASIP Journal on Wireless Communications and Networking vol. 2014, no. 1, pp. 1-10, 2014.

21. Mitra, N.J. and A. Nguyen, *Estimating surface normals in noisy point cloud data*, in *Proceedings of the nineteenth annual symposium on Computational geometry*. 2003, ACM: San Diego, California, USA. p. 322-328.

22. Tai, C.-C. and M.-C. Huang. *The processing of data points basing on design intent in reverse engineering*. 2000.

23. Menq, C. and F.L. Chen, *Curve and surface approximation from CMM measurement data.* Computers & Industrial Engineering, 1996. **30**(2): p. 211-225.

24. Anil, E.B., et al. *Assessment of the quality of as-is building information models generated from point clouds using deviation analysis*. in *Three-Dimensional Imaging, Interaction, and Measurement*. 2011. International Society for Optics and Photonics.